

Optical Engineering

SPIDigitalLibrary.org/oe

Update on linear mode photon counting with the HgCdTe linear mode avalanche photodiode

Jeffrey D. Beck
Mike Kinch
Xiaoli Sun

Update on linear mode photon counting with the HgCdTe linear mode avalanche photodiode

Jeffrey D. Beck,^{a,*} Mike Kinch,^a and Xiaoli Sun^b

^aDRS Technologies, Inc., C4ISR Group, 13544 N, Central Expressway, Dallas, Texas 75243

^bNASA Goddard Space Flight Center, Greenbelt, Maryland 20771

Abstract. The behavior of the gain-voltage characteristic of the mid-wavelength infrared cutoff HgCdTe linear mode avalanche photodiode (e-APD) is discussed both experimentally and theoretically as a function of the width of the multiplication region. Data are shown that demonstrate a strong dependence of the gain at a given bias voltage on the width of the n^- gain region. Geometrical and fundamental theoretical models are examined to explain this behavior. The geometrical model takes into account the gain-dependent optical fill factor of the cylindrical APD. The theoretical model is based on the ballistic ionization model being developed for the HgCdTe APD. It is concluded that the fundamental theoretical explanation is the dominant effect. A model is developed that combines both the geometrical and fundamental effects. The model also takes into account the effect of the varying multiplication width in the low bias region of the gain-voltage curve. It is concluded that the lower than expected gain seen in the first 2×8 HgCdTe linear mode photon counting APD arrays, and higher excess noise factor, was very likely due to the larger than typical multiplication region length in the photon counting APD pixel design. The implications of these effects on device photon counting performance are discussed. © 2014 Society of Photo-Optical Instrumentation Engineers (SPIE) [DOI: 10.1117/1.OE.53.8.081906]

Keywords: single photon counting; avalanche photodiode; HgCdTe; avalanche photodiode; mid-wavelength infrared; excess noise factor; photon detection efficiency; false event rate.

Paper 140312SS received Feb. 24, 2014; revised manuscript received Mar. 17, 2014; accepted for publication Mar. 19, 2014; published online Apr. 29, 2014.

1 Introduction

The development of the electron initiated HgCdTe linear mode avalanche photodiode (e-APD) for photon counting has continued since the last published results in 2011.¹ This first HgCdTe linear mode photon counting (LMPC) array was a success. A high single photon signal-to-noise ratio (SNR) of 13.7 was demonstrated with near 50% photon detection efficiency and 7 ns minimum time between events.² However, the original 2011 paper left some open questions which are being addressed by an NASA Earth Sciences Technology Office (ESTO) Advanced Component Technology (ACT) program out of the Goddard Space Flight Center. One of the open questions was a lower than expected gain. Another was a higher than expected excess noise factor.

Although we successfully demonstrated the linear mode photon counting with these devices, there was a discrepancy between the measured and the predicted APD gain. The SNR would have been higher at lower APD bias voltages if the actual APD gain was as high as expected based on previous gain measurements on APDs with the same cutoff wavelength. This paper explains the possible causes of the discrepancy and hopefully provides guidance to further improve the device performance.

In order to detect single photons in a linear mode APD, the ability to achieve high gains with low excess noise factor is key. The high gain is necessary to bring the typically high bandwidth impulse signal from a photon generated minority carrier up to the point where it exceeds the broadband noise of the preamp by sufficient margin to allow a high

probability of detection and with a low probability of a false detection. In addition, the excess noise factor reflects the magnitude of the variance of the gain from event to event and, in part, determines what gain is needed for a high probability of detect. For this reason, it is important to understand what affects the gain and excess noise factor in our APDs devices.

The LMPC APD gain at 13 V was about one-fifth to one-seventh of what was expected based on previous data on other HgCdTe APDs with the same cutoff wavelength (bandgap). We now believe this lower gain is due to the use of an APD design with a larger than typical multiplication region width which was implemented for the purpose of reducing diffusion jitter. As with the gain, the higher excess noise factor may also be related to the higher than typical width of the multiplication region. Here, we will describe the experimental results, and then provide our latest understanding of the basic underlying model with respect to explaining the discrepancies. The data will show that, as the multiplication width is increased, the gain at a particular bias will be lower. We then provide a deterministic gain model for the APD which predicts this behavior. In particular, the model predicts a reduction in the APD gain at a given bias voltage as the width of the multiplication region is increased. Thus, the wider multiplication regions used in these LMPC devices would explain the lower than expected gain.

Researchers at CEA/LETI have previously published a version of essentially the same model that also predicts a similar gain dependence on multiplication region width.^{3,4}

*Address all correspondence to: Jeffrey D. Beck, E-mail: jeff.beck@drs.com

Their model includes a noise model that predicts an increase in the excess noise factor as the multiplication region width is increased.³ We conclude that the lower than expected gain and higher than expected excess noise factor in our first LMPC devices seem to be explained by these models.

2 APD Gain

The APD gain of the HgCdTe APD depends primarily on the bandgap. It has been pointed out that the measured APD gain would also depend on the device geometry in cases for flood illumination where both the absorber region and the multiplication region are illuminated.⁵ This analysis predicts a multiplication region length dependence which, as shown below, is weak compared to the effect predicted by fundamental theory. The recent theoretical work, mentioned previously, predicts that the gain and excess noise factor should depend on the length of the multiplication region. Below we first present data that shows the dependence of the gain-voltage characteristic on the thickness of the n^- region, which, when fully depleted, becomes the multiplication width. We then compare the data to the predictions of the geometrical and deterministic models.

2.1 Measurement Results

The arrays that are compared all have $64 \mu\text{m}$ pitch pixels. Each pixel is composed of a 2×2 array of $32 \mu\text{m}$ pitch APDs connected together in parallel. The cutoff wavelengths are very close, near $4.3 \mu\text{m}$ at 77 K. The via diameters are $6 \mu\text{m}$. The major difference is in the diameter of the n^- region (also referred to as the “junction diameter”), shown in Fig. 1. The junction diameters are measured using a defect etch on witness slices in the same lot, and are, therefore, estimates. In the case of the typical APDs, the measured witness sample junction diameters were 15.1 to $15.5 \mu\text{m}$. For a $6 \mu\text{m}$ via with an estimated $1\text{-}\mu\text{m}$ thick surrounding n^+ region, this translates into an n^- region width, W_n , 3.5 to $3.8 \mu\text{m}$. For the LMPC case gain-voltage, data were measured on adjacent test diodes of the same geometry as the array pixels. The junction diameter was $23 \mu\text{m}$ for an estimated n^- region width of $7.5 \mu\text{m}$. The n^- region is much wider in the LMPC APD case.

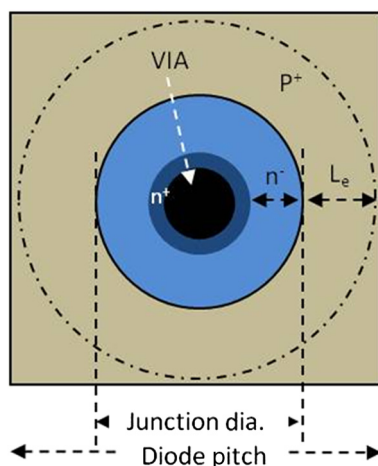


Fig. 1 Top view of avalanche photodiode (APD) unit cell showing the diode pitch, junction diameter, via, n^+ ring, n^- gain region, and collection region defined by the diffusion length (L_e), P^+ region.

Flood illuminated gain-voltage data for these devices are compared in Fig. 2. As can be seen, the extrapolated gains in the large W_n LMPC case are considerably lower at 12 V than in the other two $4.3 \mu\text{m}$ cutoff APDs. In fact, the extrapolated gain at 13 V for APD A4989-4A is 2825. This gain is a factor of five higher than the extrapolated gain of 587 for the LMPC APD. For A4989-1A, the extrapolated gain at 13 V is 4186. This gain is a factor of seven higher than the gain for LMPC APD. Also, note the difference in the threshold voltage which is defined here as the voltage at which the gain achieves a value of 2. The threshold voltage for the LMPC APD is 4.7 V which is 1.1 and 1.8 V higher than the other two cases. There is also a lower slope in the LMPC case. The lower slope will be shown to be very likely due to the fact that the depletion region did not “punch through” to the n^+ region around the via. The difference in gain between the two more typical, non-LMPC, APDs could be related to a difference in n^- region width between the two samples (A4989-1A has the smaller estimated W_n).

The same trend was seen more recently on 4×4 APDs arrays fabricated on a NASA ESTO Instrument Incubator Program (IIP), run by the Goddard Space Flight Center, which also were purposely processed to have a larger than typical junction diameter because of the larger than typical pixel size ($80 \mu\text{m}$). These APDs had a measured junction diameter on witness samples of $22.4 \mu\text{m}$ and an estimated n^- region width of $7.2 \mu\text{m}$. In Fig. 3, the gain-voltage data for a typical IIP APD is compared to an APD with a similar cutoff but junction diameter of $15.1 \mu\text{m}$ (n^- width = $3.5 \mu\text{m}$). The lower gain higher threshold voltage (3.2 V compared to 2.9 V) in the larger junction diameter device is apparent. At high biases, the slopes are approximately the same.

On the NASA ACT program, we have recently fabricated a 2×8 LMPC lot, A8327, which shows similar dark current and gain performance to the first LMPC lot, A7164. As with A7164, the lot was processed to have large junction diameters in the neighborhood of $23 \mu\text{m}$. The actual junction diameters measured on witness samples came out lower: 20 to $22 \mu\text{m}$. The gain-voltage data, shown in Fig. 4, indicate a threshold voltage of 3.45 V and a gain at 13 V of around 1900. The lower threshold voltage and higher gain compared to lot A7164 are apparent. The gain normalized dark current

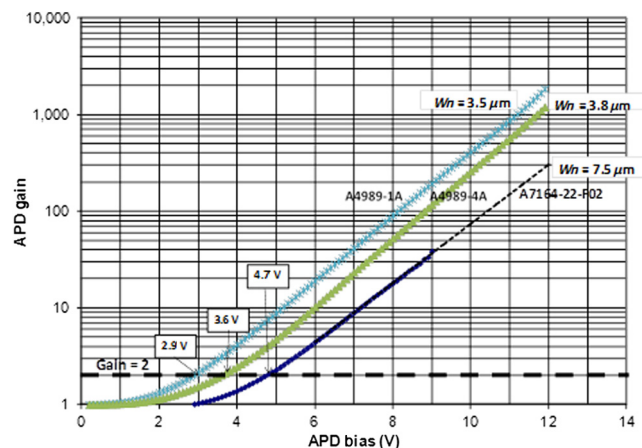


Fig. 2 Flood illumination gain-voltage data on two typical $4.3 \mu\text{m}$ cutoff HgCdTe $32 \mu\text{m}$ pitch APDs at 80 K compared to the LMPC fanout pixel gain data. The gain = 2 threshold voltages are indicated.

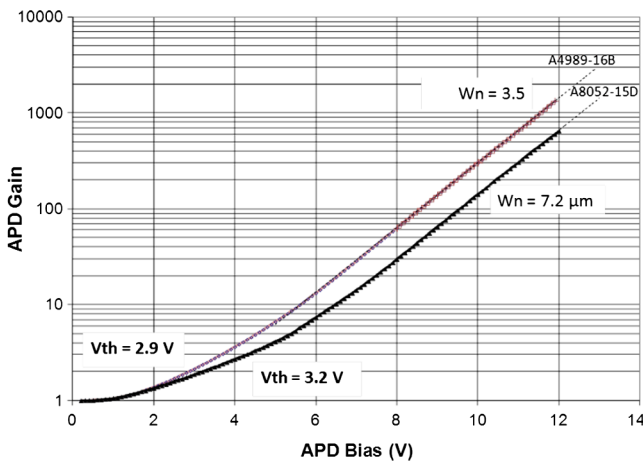


Fig. 3 Flood illumination gain-voltage data on 15 μm junction diameter APD ($W_n = 3.5 \mu\text{m}$) and a 22.4- μm diameter APD ($W_n = 7.2$). The gain = 2 threshold voltages are indicated.

versus APD gain is plotted in Fig. 5. The gain normalized at a gain of 1000 is around 1 fA corresponding to an input dark electron rate of 6000 electrons/s. The gain normalized dark current remains <5 fA (<30 ke/s) out to a gain of 1900.

In conclusion, our APD gain versus voltage data show a dependence of gain on junction diameter. We next discuss two explanations for why the gain depends on the junction diameter.

2.2 Geometry Effect

The geometry effect on gain arises from the way the gain is measured, and the fact that the effective optical collection area of the cylindrical APD is a function of the APD gain. The gain is typically measured under flooded illumination conditions. The photosignal is measured as a function of bias. The measured gain is the ratio of the photosignal at high bias to the photosignal at low bias where the gain is unity (where the signal is bias independent). We assume the top side illuminated cylindrical diode architecture, see Fig. 1, in which both the central n-region and the surrounding p-region are flood illuminated. We typically assume also that the hole and electron diffusion lengths are larger than

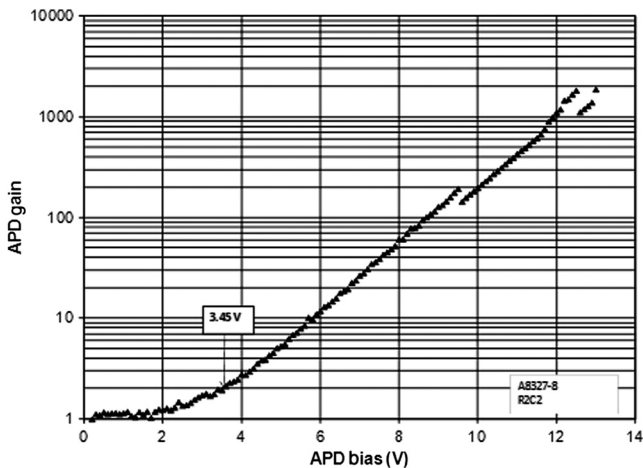


Fig. 4 Gain versus voltage data on A8327-8 (the cause of the gain discontinuities in the data is not known at the present time).

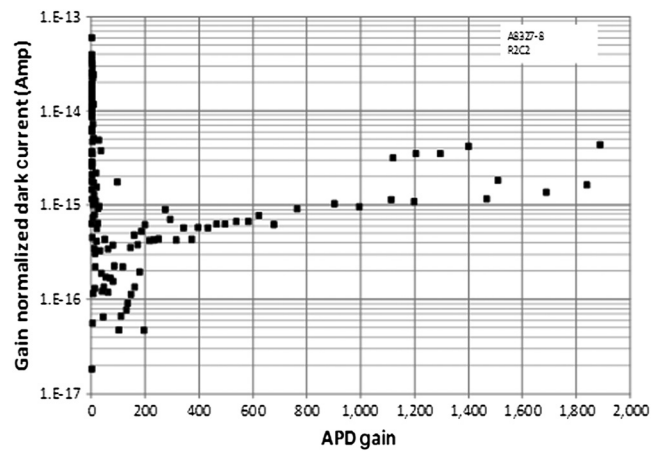


Fig. 5 Gain normalized dark current versus gain on A8327-8.

the dimensions of the n- and p-regions. We assume the diodes are in a two-dimensional array of equally spaced cylindrical APDs, in an orthogonal arrangement, where the area of the p absorber region is determined by the inter-diode pitch and the diameter of the n-region. This is a valid assumption if the diffusion lengths of the hole on the n-side and the electron on the p-side are larger than the width of the n-region in the case of the hole, or the interjunction distance in the case of the electron. In the low bias, unity gain, region both the n- and p-regions contribute to the signal in proportion to their effective areas in the pixel. In this case, assuming long hole and electron diffusion lengths, the collection area is the entire pixel except for the via (Fig. 1). If the electron diffusion length, L_e , is smaller than junction separation, then the absorption region will be confined to the ring of width L_e around the n^- region, as shown by the dashed line in Fig. 1. At high gains, the signal contribution from the n-side (the multiplication region) becomes almost negligible compared to the contribution of signal from the p-side which is fully gained. Thus the measured gain does not reflect the true gain but somewhat lower gain due to the optical fill factor. It can be shown that the measured gain M_{measd} at high gains is approximately equal to the true gain M times the ratio of the APD mode fill factor FF_p (effective p-region area) to the unity gain fill factor FF_{ug} . The approximation neglects the optical signal generation in the multiplication region which is small due to the very rapid reduction in gain moving in from the junction boundary and the relatively small area of the gain region itself

$$M_{\text{measd}} = \frac{FF_p \cdot M}{FF_{\text{ug}}} \tag{1}$$

The typical 32 μm pitch 2×2 APD 64 μm pitch pixels have junction diameters from 15 to 18 μm while the LMPC pixel, in order to minimize jitter and maximize electron collection efficiency (eCE), had a junction diameter of about 23 μm . These differences and their effect on the ratio of the measured gains are tabulated in Table 1. As can be seen, the expected gain reduction, based on the geometry, is small compared to the measured differences in gain seen in Fig. 2.

The LMPC array, which was fabricated on vacancy doped HgCdTe, should have had a shorter effective electron diffusion length (e.g., 5 μm) than the other devices in Fig. 2 which

Table 1 Geometry factors for the 4.3 μm cutoff devices compared in Fig. 2. These calculations assume that the hole and electron diffusion lengths are long enough for 100% collection in the n- and p-regions, respectively, as defined by the pixel geometry.

Device	Diode pitch (μm)	Estimated junction diameter (μm)	Estimated n^- region width W_n (μm)	Unity gain fill factor	APD fill factor	Normalized gain reduction factor (FF_p/FF_{ug})
A4989-1A	32	15.05	3.5	0.911	0.765	1.0 ^a
A4989-4A	32	15.45	3.8	0.911	0.756	0.99
LMPC-22-RO2	32	23.0	7.5	0.972	0.594	0.73

^aNormalization reference.

were fabricated on copper doped HgCdTe. In this case, the collection area on the p-side would be determined by the diffusion length. We calculated an estimated gain factor in which the collection area on the p-side is limited by the theoretical diffusion length of 5 μm . This reduces the measured gain even further since the area of the APD collection region is reduced relative to the area of the n-region. In the case of a 5 μm diffusion length, the gain of the LMPC pixel is expected to be about 61% of the gain for the 15- μm diameter junction copper doped APDs in Fig. 2. Even in this case, the expected gain reduction factor of 0.6 is much less than seen experimentally. The calculation results for the diffusion length limited case are summarized in Table 2.

In conclusion, the geometry effect, while predicting a reduced measured gain due to a larger junction diameter, cannot explain the much larger discrepancy between the gain seen in the wide n^- region LMPC APD and the gain seen in APDs with narrower n^- regions.

2.3 HgCdTe APD Physics Predictions for Gain Dependence on Multiplication Region Width

A multiplication region width dependence on gain and excess noise factor were first reported by Perrias et al.⁶ Then Rothman published a paper which proposed a history-dependent model³ based on the ballistic model of Kinch⁷ and the Shockley lucky electron model⁸ to explain this behavior. The ballistic model of Kinch predicts a multiplication region width dependence on gain as will be described below.

The physics of avalanche multiplication as applied to HgCdTe has evolved over the years, since it was first applied to LWIR material by Elliott et al.⁹ in the 1989 US II-VI Workshop. Essentially $k = 0$ noiseless gains in excess of 1000 for mid-wavelength infrared (MWIR) HgCdTe have been reported by many groups,¹⁰⁻¹² where k is the hole to electron ionization ratio. A ballistic electron theory^{3,4,7} has been developed in an attempt to model the

experimental data for LWIR, MWIR, and SWIR HgCdTe e-APDs, with some degree of success. Shockley's lucky electron model is the preferred approach for APDs fabricated on MWIR and LWIR cutoff HgCdTe, and can be set up in one of two ways, namely (1) with an arbitrary number of adjustable parameters, which enable a fit to experimental data, or (2) by appealing to the physics of the problem, with the introduction of real world parameters whose values should be consistent not only between themselves but also with other transport measurements of the material. An example of the second approach is the ballistic transport model of the lucky electron as discussed by Brennan,¹³ but now modified to allow for a Kane-type non-parabolic conduction band. The resulting expression for the electron ionization coefficient is given by

$$\alpha = \frac{qF}{E_{th}} \exp\left[\frac{-E_{th}}{qF\tau} \sqrt{\frac{2m_o^*}{qE_g}}\right], \quad (2)$$

where q is the charge of an electron, E_g is the bandgap, m_o^* is the effective mass of the electron at the conduction band minimum, F is the applied field, τ is the relevant lifetime for momentum scattering of the electron, and E_{th} is the threshold energy for impact ionization. The pre-exponent term is merely the inverse of the ionization mean free path, λ_{th} , where $E_{th} = qF\lambda_{th}$, and the exponent represents the probability of the electron traveling for a time sufficiently long as to enable impact ionization, relative to the momentum scattering lifetime, τ . The avalanche gain for an e-APD with depletion width W , in a uniform electric field V/W , is thus given by

$$\begin{aligned} G &= \exp(\alpha W) = \exp\left[\frac{qV}{E_{th}} \exp\left(\frac{-2E_{th}W}{qV\tau} \sqrt{\frac{m_o^*}{2qE_g}}\right)\right] \\ &= \exp\left[\frac{qV}{E_{th}} \exp\left(\frac{-2E_{th}W}{qV\lambda}\right)\right], \end{aligned} \quad (3)$$

Table 2 Geometry factors for the 4.3 μm cutoff devices compared in Fig. 2 where the collection area on the p-side is limited by the diffusion length.

	Junction diameter (μm)	Diffusion length L_e (μm)	Via radius (μm)	Assumption	Measured gain at true gain of 1000	Normalized gain reduction factor
Copper doped	15	13	3	L_h, L_e large-square geometry	885	1.0 ^a
Vacancy doped	23	5	3	L_h large, L_e small-cylindrical geometry	532	0.601

^aNormalization reference.

where we have substituted for the high energy saturation velocity $v_{\text{sat}} = [2qE_g/m_o^*]^{1/2}$, providing a momentum destroying mean free path $\lambda = v_{\text{sat}}\tau$. The gain, under these conditions, is seen to be dependent on the threshold energy E_{th} , whereas the threshold voltage, i.e., the applied voltage at which the gain is two, will be determined by both the threshold energy, and the ratio of (W/λ) . E_{th} will depend directly on the semiconductor bandgap at the specific operating temperature, and if elastic scattering is involved, will also be affected by a degree of energy dispersion. The ratio of the multiplication region width to the mean free path (W/λ) is where the gain dependence on multiplication width comes from and reflects how many times the electron will be scattered on its way across the multiplication region. This dependence makes sense intuitively and also suggests a reason for the predicted increase in excess noise factor as W increases,³ as scattering events would be expected to remove, at least partially, the deterministic nature of the gain process.

Figure 6 illustrates the predicted dependence of gain on bias voltage as a function of multiplication region width at 77 K for a 4.3 μm cutoff for a mean free path of 3.2 μm . The assumed value of E_{th} is $4.5E_g$ at the operating temperature in approximate agreement with early impact ionization theory for MWIR HgCdTe. The predicted gains are in the range displayed by the data of Figs. 2 and 3. For the cases we are considering, if we assume a 6 μm via with a 1 μm n^+ region, the n^- region width in the case of the D4989 samples is about 3.5 to 3.8 μm for a predicted gain of near 3000 at 13 V from Fig. 6 which is consistent with the data shown in Figs. 2 and 3. For the LMPC case, the n^- region width is about 7.5 μm for a 23- μm diameter diode for a predicted gain near 500, a factor of about 6 lower. In conclusion, the factor of 5 to 7 difference in high bias gain between the LMPC APD and the other APDs is explained by the theoretical model of Kinch for the HgCdTe APD. Obviously, the above analysis involves several approximations. Nevertheless, it indicates trends which are in good agreement with the experimental results.

We would expect both the physics explanation and the geometrical effect to come into play for the flood illumination measurements. Note that the physics model is calculating what is defined as the true or fundamental gain, while the

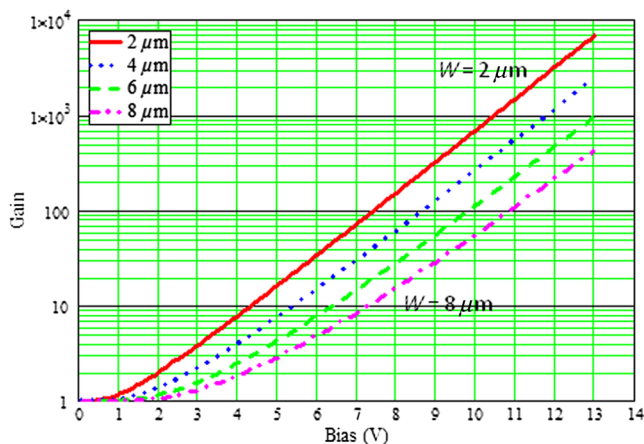


Fig. 6 Gain-voltage calculation using Kinch model with fixed multiplication region widths from 2 to 8 μm . (for 4.3 μm cutoff HgCdTe, $\lambda = 3.2 \mu\text{m}$).

geometrical model is calculating a correction to the measured gain for the flood illumination case.

The model was updated to take into account the fact that the multiplication width W depends on bias until the depletion region reaches the n^+ region, see Fig. 1. We also added in the geometrical effect discussed above with the approximation that neglects gain in the n-region. The inclusion of the varying W effect to the model should more accurately predict the behavior of the turn-on region when the multiplication region length is still changing with bias. The updated model predictions for gain versus bias for an n^- region doping of $4 \times 10^{14} \text{ cm}^{-3}$ are plotted in Fig. 7. Figure 7 reveals the expected difference in behavior at low bias. It also reveals an increase in the exponential slope at intermediated voltages corresponding to the point at which the depletion region reaches the n^+ region and stops growing. This change in slope has been seen experimentally, for example see Fig. 3. In the high bias regime, beyond punch-through the slopes are close to identical, as expected. Notice that in Fig. 7 that punch-through has not occurred up to 13 V for the 8- μm wide n^- region case. It is possible that this was the case for the LMPC device shown in Fig. 2. This would explain the lower slope out to 13 V. Figure 7, which represents the predicted “measured gain,” as expected, shows lower gains due to the geometry effect. The predicted gains are within the range of the measured data.

2.4 Excess Noise Factor

Researchers at CEA/LETI have developed the HgCdTe APD theory to the point whereby it predicts an excess noise factor dependence on the multiplication width.³ This would be expected as the width becomes larger than the mean free path between scattering events. Even though single carrier ionization behavior is probably not significantly affected, scattering would be expected to at least partially remove the deterministic (history-dependent) nature of the process. Indeed, experimental data showing this dependence has been published.^{3,14}

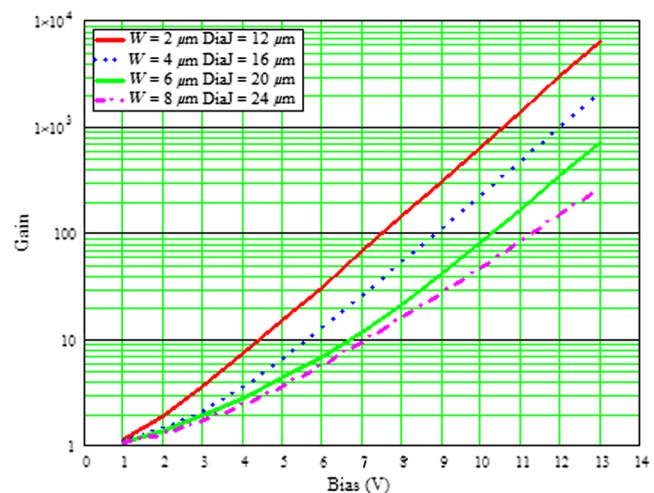


Fig. 7 Gain-voltage for bias-dependent multiplication region widths from 2 to 8 μm (for 4.3 μm cutoff HgCdTe at 77 K with $N_D = 4 \times 10^{14} \text{ cm}^{-3}$, $\lambda = 3.2 \mu\text{m}$).

3 Discussion

The lower than expected gain at a given bias can often be compensated for by increasing the bias voltage. Indeed, the first LMPC array achieved very good performance in spite of the fact that the required bias was 2 to 3 V higher than expected. In general, it is likely that requiring a larger bias to achieve a required gain would reduce device yield. In fact, as the bias gets higher, issues associated with defective pixels become more problematic with regard to focal plane array operation. In addition, lower bias voltage is even more important for short cutoff HgCdTe APDs for which the required biases are often prohibitively high from a readout integrated circuit compatibility standpoint. Also, higher linear mode gain is desirable in terms of being able to meet sensitivity requirements with good margin. Finally, the use of a narrower multiplication region in the HgCdTe APD is expected to reduce the excess noise factor. For the HgCdTe photon counting pixel, higher gains and lower excess noise factor (with lower jitter and higher electron collection efficiency) are expected to be achieved by reducing both the n- region width and the APD pitch.

4 Summary

The accompanying paper “Linear mode photon counting with the noiseless gain HgCdTe e-APD,”¹ reported on the first single photon sensitive detectors in the near-infrared to MWIR wavelength range. In this update to that paper, the lower than expected gain and the higher than expected excess noise factor in the linear mode photon counting HgCdTe APD^{1,2} has been attributed to the wider than usual multiplication region width used in the particular design for this detector. We showed data on a number of APDs that strongly indicated the gain dependence on multiplication region width. We then showed that the deterministic model of Kinch⁷ predicts this dependence. Our results corroborate the experimental findings and theoretical work of Rothman.³

The deterministic model for APD gain was extended to take into account the geometrical effects and the effect of the varying multiplication region width as a function of APD bias in the low bias region. These modifications are expected to better reflect the measured gain of our APDs.

References

1. J. Beck et al., “Linear mode photon counting with the noiseless gain HgCdTe e-APD,” *Proc. SPIE* **8034**, 80330N (2011).
2. A. Gleckler et al., “Application of an end-to-end linear mode photon counting (LMPC) model to noiseless-gain HgCdTe APDs,” *Proc. SPIE* **8033**, 80330O (2011).
3. J. Rothman et al., “History dependent impact ionization theories applied to HgCdTe e-APDs,” *J. Electron. Mater.* **40**(8), 1757–1768 (2011).
4. J. Rothman et al., “Short-wave infrared HgCdTe avalanche photodiodes,” *J. Electron. Mater.* **41**(10), 2928–2936 (2012).
5. J. Beck et al., “Performance and modeling of the MWIR HgCdTe e-APD,” *J. Electron. Mater.* **38**(8), 1579–1592 (2009).
6. G. Perrias et al., “Gain and dark current characteristics of planar HgCdTe avalanche photo diodes,” *J. Electron. Mater.* **36**(8), 963–970 (2007).
7. M. Kinch, “A theoretical model for the HgCdTe electron avalanche photodiode,” *J. Electron. Mater.* **37**(9), 1453–1459 (2008).
8. W. Shockley, “Problems related to p-n junctions in silicon,” *Solid State Electron.* **2**(1), 35–60 (1961).
9. C. T. Elliott et al., “Reverse breakdown in $\text{Cd}_x\text{Hg}_{1-x}\text{Te}$ diodes,” *J. Vac. Sci. Technol. A* **8**, 1251–1253 (1990).
10. J. Beck et al., “Gated IR imaging with 128×128 HgCdTe electron avalanche photodiode FPA,” *Proc. SPIE* **6542**, 654217 (2007).
11. G. Perrais et al., “Impulse response time measurements in $\text{Hg}_{0.7}\text{Cd}_{0.3}\text{Te}$ MWIR avalanche photodiodes,” *J. Electron. Mater.* **37**(9), 1261–1273 (2008).
12. M. B. Reine et al., “Characterization of HgCdTe MWIR back-illuminated electron-initiated avalanche photodiodes,” *J. Electron. Mater.* **37**(9), 1376–1386 (2008).
13. K. F. Brennan, *Physics of Semiconductors*, p. 513, Cambridge University Press, Cambridge, UK (1999).
14. G. Vojetta et al., “Linear photon-counting with HgCdTe APDs,” *Proc. SPIE* **8375**, 83750Y (2012).

Jeffrey D. Beck received SM and SB degrees in electrical engineering from MIT, Cambridge, Massachusetts, in 1972. He joined Texas Instruments in 1978 and was elected Distinguished Member of Technical Staff in 1996. He received the MSS Herschel Award on behalf of DRS in 2004 for his discovery of the noiseless gain HgCdTe APD. He was elected an MSS fellow in 2006. He won the international “2009 Innovation Award” from Finmeccanica S.p.A, Italy. He is currently a staff scientist at DRS Technologies, Dallas, Texas.

Mike Kinch received his PhD in physics from Oxford University, England. He joined Texas Instruments in 1966 and was elected a TI fellow in 1985. He has published seminal papers and written books on all facets of IR technology. He was a recipient of the 1987 IEEE Jack A. Morton Award, the 2008 MSS Henry Levinstein Award, elected a fellow of the APS in 1988, and the MSS in 2002. He is currently a vice president of DRS Technologies in Dallas, Texas.

Xiaoli Sun received his PhD in electrical engineering from Johns Hopkins University, Baltimore, Maryland, in 1989. He has been the detector lead and instrument scientist for lidar on NASA’s Mars Global Surveyor, ICESat, MESSENGER, and Lunar Reconnaissance Orbiter (LRO) missions. He also led the first lunar laser communication experiments from Earth to LRO in 2012. He is currently a research scientist at the Solar System Exploration Division at NASA’s Goddard Space Flight Center, Greenbelt, MD.